Spontaneous Pattern Formation on Ion Bombarded Si(001)

Jonah Erlebacher and Michael J. Aziz
Harvard University, Division of Engineering and Applied Sciences, Cambridge, Massachusetts 02138

Eric Chason, Michael B. Sinclair, and Jerrold A. Floro
Sandia National Laboratories, Albuquerque, New Mexico 87185

(Received 2 November 1998)

Spectroscopic light scattering was used to monitor periodic ripple evolution on Si(001) *in situ* during Ar^+ sputtering. Analysis indicates that under high flux the concentration of mobile species on the surface is temperature and ion flux independent. This is due to an effect of ion collision cascades on the concentration of mobile species. We thereby measure the migration energy on the surface to be 1.2 ± 0.1 eV. The technique is generalizable to any material, including high temperature and insulating materials for which surface migration energies are notoriously difficult to measure. [S0031-9007(99)08687-1]

PACS numbers: 68.35.Bs, 81.10.Aj, 85.40.Ux

Low-energy (500–1000 eV) ion bombardment is a common technique used in many thin film applications such as forming shallow junctions, sputter etching and deposition, ion beam assisted growth, reactive ion etching, and plasma assisted chemical vapor deposition. Under certain conditions, ion sputtering is known to produce patterns on surfaces. Features such as ripples, bumps, or cones are common [1–3]. Typical length scales of these features are of the order of 10–1000 nm. In some cases, these features are nuisances, such as in sample thinning for transmission microscopy or depth profiling by secondary ion mass spectroscopy. However these nanoscale patterns also hold promise in applications as varied as optical devices, templates for liquid crystal orientation, and strain-free patterned substrates for heteroepitaxial growth of quantum dots or wires. Rippling has been observed in amorphous materials ($\mathrm{SiO_2}$ [1]), metals (Ag [4]), and semiconductors (Ge [5], Si [6], and others).

In this study, a recently developed *in situ* light scattering spectroscopic technique [7] was used to monitor ripple evolution on Si(001) during Ar^+ sputtering. The technique allowed the first systematic study of the temporal and spatial evolution of both ripple wavelength and ripple amplitude as functions of both temperatures and ion beam flux. Theoretical models describe rippling as arising from competition between ion beam roughening/etching and surface diffusion or viscous flow mediated relaxation [8]. Our results here help illuminate the range of validity of these models. Additionally, we describe the method by which the activation energy for surface migration can be found. A salient feature of these experiments was our use of a very high ion flux compared to other rippling experiments. At high fluxes, the annihilation process for mobile species becomes dominated by collision cascades. Sputter-induced rippling can, in principle, occur on the surface of any material. As such, it holds great promise as a method for measuring the activation energy for surface migration on high temperature or insulating materials, which are generally notoriously difficult to measure.

Rippling experiments were performed on Si(001) (p type, 3–10 Ω cm) in an ultrahigh vacuum chamber (base pressure of 2×10^{-10} Torr). Ions bombarded the surface at a glancing incidence, 67.5° from normal, with an energy of 750 eV; the projected ion beam ran along the [110] direction [9]. Previous studies of sputter rippling have used *in situ* x-ray scattering [1,2], which measured the rms roughness averaged over the surface, or *ex situ* microscopy [4]. We used a recently developed *in situ* UV spectroscopic technique, light scattering spectroscopy (LiSSp), that measures the scattered light spectrum in a fixed direction [7]. A broadband 150 W Xe arc lamp illuminated the surface during sputtering; a solid state spectrometer collected nonspecular scattered light. The spectrometer response was sufficient to measure spatial features between 200 and 2000 nm, depending on the relative orientation of the illumination and collection optics. For each measured spectrum, a background spectrum without Xe illumination was also measured to (1) subtract effects of thermal radiation from the UV scattered spectrum and (2) measure temperature [10].

LiSSp has major advantages over the other methods. The entire scattered light spectrum is acquired, so diffraction peak positions, widths, and amplitudes were simultaneously obtained for all relevant feature sizes. Also, by using spectroscopic detection, the need to rotate or move the sample during the measurements is removed. For these reasons, data collection was significantly simplified and a wider range of parameters could be studied. The power spectral density (PSD) of the sample surface (i.e., the square of the magnitude of the Fourier transform of the surface profile or, equivalently, the surface height-height autocorrelation function) was extracted directly from the measured scattered light spectrum following the analysis in Ref. [11].

To illustrate the effectiveness of the technique, Fig. 1 shows the PSD of a rippled sample collected *in situ* at 555 °C. The PSD determined from light scattering spectrum is overlayed with the PSD as measured *ex situ* using antiferromagntic (AFM) (square symbols) [12]. The peak in the PSD corresponds to a ripple wavelength of 360 nm and an amplitude of 11 nm, illustrating the sensitivity of the technique. The AFM micrograph of the surface showing the ripples is displayed in the figure inset.

For the ion current of 0.7 mA/cm^2, rippling was monitored over the temperature range 500–600 °C. Figure 2 shows the PSD evolution for a representative example. The projected directions of the ion beam and scattering vector for the optical spectroscopy were perpendicular to each other, as shown in Fig. 1. In the direction parallel to the projected ion beam no significant roughening was observed [13]. The spectra shown were collected *in situ* at intervals of 500 sec. Three features can be seen in Fig. 2 and were generally observed for all data: (i) For large spatial frequencies (above ~ 0.02 nm^{-1} in Fig. 2), roughness does not increase, (ii) roughness grows at all spatial frequencies below this cutoff, and (iii) there is a fastest growing spatial frequency q^* whose value is independent of time and dominates all other frequencies at long times. The ripple wavelength, λ^* (570 nm in Fig. 2), is simply $2\pi/q^*$.

The foundation of most theories of ion rippling is due to Bradley and Harper (BH) [8]. Theirs is a linear stability analysis of a surface undergoing roughening due to sputtering, on the one hand, and annealing by surface diffusion, on the other. Here we summarize the salient points. Consider an ion beam impinging on a surface at an angle θ, measured from normal. A theory of sputter yield due to Sigmund [14] leads to a roughening term that is proportional to the curvature of the surface in the direction perpendicular to the ion beam κ. For annealing, mass transport via surface diffusion leads to a relaxation term proportional to the second spatial derivative of κ [15]. In the moving reference frame of the sputtered surface, the change in average height with time, $\partial h/\partial t$, can be written

$$\frac{\partial h}{\partial t} = S\kappa + B\frac{\partial^2}{\partial s^2}\kappa\,, \qquad (1)$$

where the derivatives are taken with respect to the surface arc length s measured perpendicular to the beam. Under the near-glancing conditions used here, the roughening prefactor is given by $S = -(fa/n)Y_0(\theta)\Gamma_2(\theta)$, where f is the ion flux, a is the average depth of ion energy deposition, n is the atomic volumetric density, $Y_0(\theta)$ is the (incidence angle dependent) sputter yield, and $\Gamma_2(\theta)$ is a coefficient governing the erosion rate dependence on the local surface curvature. The relaxation prefactor is given by $B = D_s C\gamma/n^2 k_B T$, where γ is the surface energy per area, T is the temperature, k_B is Boltzmann's constant, D_s is the surface diffusivity, and C is the concentration (number/area) of mobile species that participates in surface diffusion. Equation (1) is generally valid when $a\kappa \ll 1$, which was always satisfied in our experiments.

In the limit of short times and small slopes (infinitesimal amplitudes), one makes the approximation $\kappa \approx \partial h^2/\partial x^2$. In this case, Eq. (1) can be solved by Fourier techniques. Specifically, each component, $h_q(t)$, of the surface spatial frequency spectrum grows exponentially with the rate constant $R_q = Sq^2 - Bq^4$. There is a maximal value of R_q, indicating that there is a fastest growing spatial frequency, q^*, independent of time and given by

$$q^* = (S/2B)^{1/2}. \qquad (2)$$

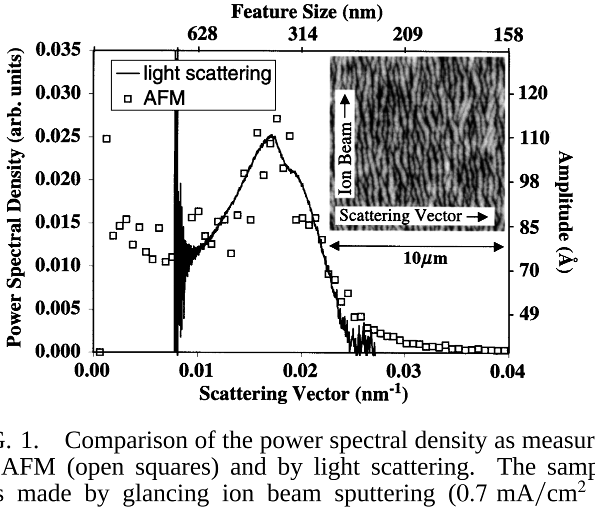

FIG. 1. Comparison of the power spectral density as measured by AFM (open squares) and by light scattering. The sample was made by glancing ion beam sputtering (0.7 mA/cm^2 at 67.5° from normal) at a sample temperature of 555 °C for 8500 sec. The small discrepancy near 0.025 nm^{-1} is due to both AFM pixelation error and spectrometer cutoff. Inset: AFM topograph of this sample showing the projected ion beam direction and the direction of light scattering for the optical spectroscopy.

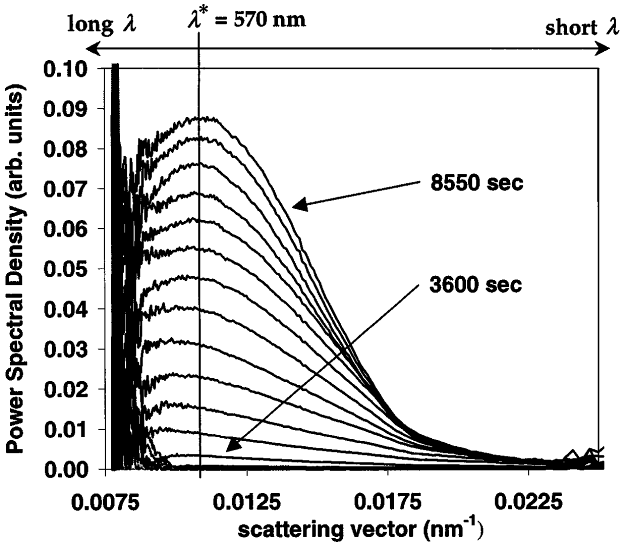

FIG. 2. Example of the temporal evolution of the ripple morphology: $T = 582$ °C, $\lambda^* = 570$ nm. Curves are measured PSD at intervals of approximately 500 sec. The PSD of the fastest growing frequency is not necessarily the greatest at early times due to a nonuniform initial roughness spectrum.

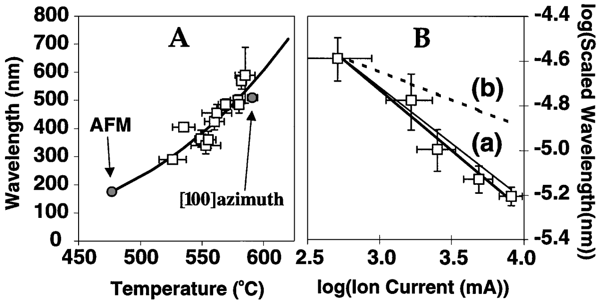

FIG. 3. (A) Measured critical wavelength, λ^* vs sample temperature (squares), and a fit to the prediction of the Bradley-Harper theory (line). (B) Scaled critical wavelength vs ion beam current (out of gun): data (squares); thick line: power law fit, $\lambda^* \propto f^{-0.54}$; (a), thin line: power law, $\lambda^* \propto f^{-1/2}$; (b), dotted line: power law, $\lambda^* \propto f^{-1/4}$.

These conclusions are consistent with our observations (i)–(iii) above.

Figure 3(A) shows the dependence of the ripple wavelength on temperature at fixed ion flux. The only unknown in Eq. (2) defining q^* is the product $D_s C$, contained in B [16]. Using the Arrhenius form, $D_s C = A \exp(-\varepsilon / k_B T)$, we obtain a good fit of the data to Eq. (2) with best fit parameter values $A = 3.5 \times 10^{10}\ \mathrm{sec}^{-1}$ and $\varepsilon = 1.2 \pm 0.1$ eV. The data are shown in the figure as open squares and the fit as a line.

If D_s and C are both thermally activated and C is equal to its value in equilibrium, then ε would represent the sum of a migration energy for diffusion, E_M, and a creation free energy for the diffusing species, E_F. This sum can be measured by thermal annealing experiments in which lithographically patterned rippled surfaces are heated and their amplitude decay is monitored. For experiments on Si(001), Keeffe *et al.* [17] found $E_M + E_F = 2.4$ eV, significantly larger than our measured value for ε. In fact, our measured value $\varepsilon = 1.2 \pm 0.1$ eV is identical, within experimental error, to the migration energy, $E_M = 1.1 \pm 0.1$ eV, for diffusion of dimers on Si(001) measured by STM [18]. A recent measurement by Tromp *et al.* indicates that $E_F = 0.35$ eV [19], which is interesting in its inconsistency with the combination of the Keeffe and STM results, but is still so large that numerical comparison of our value with the others makes sense only if we interpret ε as a migration energy alone. This fact suggests that C in our experiment is not thermally activated at all. Furthermore, Tromp *et al.* show that the mobile species on the Si(001) surface at the temperatures relevant here are dimers and not single adatoms, supporting the idea that ε is the activation energy for surface diffusion of a dimer. For these reasons, we refer to the mobile species as the addimer.

The steady-state concentration of addimers is governed by a balance of their creation and annihilation rates. In the simplest picture, addimers are created at a rate equal to $f Y_1$, where f is the ion flux and Y_1 is the number of addimers created per incident ion. Usually, only annihilation mechanisms involving thermally activated diffusion are considered to be operative. These can be either addimer-addimer aggregation into stable islands or addimer diffusion to traps such as step edges or surface vacancies. A previously unconsidered third possibility is that addimers are directly removed by impinging ions. This process is athermal and the annihilation rate is equal to $f C \sigma_c$, where the cross section σ_c is related to the area at the surface over which an ion's damage is deposited in the collision cascade. An impinging ion resets a surface patch of area σ_c to an addimer concentration that is independent of T and its value before the collision.

We write the net creation rate of addimers as

$$dC/dt = f Y_1 - f C \sigma_c - C/\tau_1 - 2C^2/\tau_2 , \qquad (3)$$

where τ_1 is the characteristic time for an addimer to diffuse to a step or other surface trap, and τ_2 is the characteristic time for two addimers to impinge. If the annihilation rate is dominated by direct removal by ion collision cascades, then the steady-state concentration is $C_{\mathrm{ss}} = Y_1/\sigma_c$, independent of f and T, and leads via Eq. (2) to $\lambda^* \propto f^{-1/2}$. For addimer-addimer dominated kinetics, Eq. (3) becomes $dC/dt = f Y_1 - (2C)(4D_s/a_0^2)(C/C_{\mathrm{site}})\sigma_1$, where a_0 is the surface lattice parameter, C_{site} is the concentration of surface sites, and σ_1 is dimensionless capture cross section (the so-called monomer capture number). Identifying $\tau_2 = a_0^2 C_{\mathrm{site}}/4D_s\sigma_1$ yields $C_{\mathrm{ss}} \propto \sqrt{f/D_s}$, which in turn leads to $B(T) \propto \gamma\sqrt{f D_s}/k_B T$ and $\lambda^* \propto f^{-1/4}$. For trap-dominated kinetics, $C_{\mathrm{ss}} = f Y_1 \tau_1$. The temperature dependence of τ_1 is clarified by writing it in terms of a characteristic length between traps, $l_{\mathrm{trap}} = \sqrt{D_s \tau_1}$. In steady state, l_{trap} does not change with time. This implies $C_{\mathrm{ss}} \approx (f/D_s) l_{\mathrm{trap}}^2$, which in turn leads to $B(T) \approx f\gamma/k_B T$ and a flux-independent ripple wavelength.

To summarize, the differing scenarios for the steady-state concentration of adatoms yield the following variations of ripple wavelength with flux and temperature:

$$\text{(a) Ion cascade annihilation:}\quad \lambda_1^* \approx f^{-1/2}(kT/\gamma)^{-1/2}\exp(-E_M/2k_B T), \qquad (4a)$$

$$\text{(b) Addimer-addimer annihilation:}\quad \lambda_2^* \approx f^{-1/4}(kT/\gamma)^{-1/2}\exp(-E_M/4k_B T), \qquad (4b)$$

$$\text{(c) Surface trap annihilation:}\quad \lambda_3^* \approx (kT/\gamma)^{-1/2}. \qquad (4c)$$

It follows that the dominant annihilation mechanism is identified by measuring the flux dependence of λ^*.

The positive slope of the data shown in Fig. 3(A) dismisses case (c). Cases (a) and (b) have the same temperature dependence, of the form $(kT)^{-1/2}\exp(-E/k_B T)$, but different flux dependencies. We have measured λ^* at different fluxes, but also at different temperatures. However, we can scale out the temperature dependencies of cases (a) and (b) by multiplying the λ^* values obtained at the various temperatures by $(kT)^{-1/2}\exp(-E_M/2k_BT)$ for case (a) and by $(kT)^{-1/2}\exp(-E_M/4k_BT)$ for case (b). Figure 3(B) shows the flux dependence of the critical wavelength as a result of this scaling. Case (a), $\lambda^* \propto f^{-1/2}$, is the only one consistent with the data, and we conclude that we have reached a steady-state concentration of mobile species that is both flux and temperature independent. This result is surprising, and is contrary to the usual picture of sputtering, in which the number of surface defects such as addimers increases with flux [20]. Plugging in reasonable values into Eq. (3) for all relevant quantities also supports this conclusion. We do not claim that the dynamic structure of a surface undergoing ion bombardment is always temperature and flux independent. We suggest, rather, that at a sufficiently long time at a sufficiently high flux or low temperature, the mobile species concentration saturates at a value that depends only on the character of the ion/material interaction, i.e., the parameters Y_1 and σ_c. This prediction can be further tested by repeating the experiment with differing ion energies.

An assumption of BH theory is that the surface energy does not change with local surface orientation, an anisotropy that will tend to suppress, or at least strongly modify, ripple instabilities. For amorphous solids this assumption is reasonable, but for monocrystalline Si well below the thermodynamic roughening temperature, it is somewhat surprising that our results follow BH so well. One possibility is that this effect is negligible for small amplitude to wavelength ratios. Another possibility is that conditions of high addimer supersaturation effectively reduce surface energy anisotropy, thereby making it possible to observe roughening instabilities in nominally anisotropic systems, as was recently suggested by Jesson *et al.* [21], using a result from Nozieres and Gallet [22].

In summary, we have characterized the temperature and ion beam flux dependence of the sputter rippling phenomenon on Si(001). The flux dependence of the ripple wavelength, in particular, leads us to conclude that under high flux ion bombardment the steady-state concentration of mobile species on the surface is flux and temperature independent. This previously unobserved result means the dominant annihilation process of mobile surface species is direct removal by ion collision cascades. This process may play an important role in governing film quality during ion-assisted epitaxial growth of thin films. It also permits a straightforward measurement of the surface migration energy, which for Si(001) we find to be 1.2 ± 0.1 eV over the temperature range of 500–650 °C.

The authors acknowledge stimulating discussions with Sean Hearne and Craig Arnold, and technical advice given by John Hunter. This work was supported by DE-FG08-89ER45401. Portions of this work were performed at Sandia National Laboratories, supported by the United States Department of Energy under Contract No. DE-AC04-94AL85000.

[1] T. M. Mayer, E. Chason, and A. J. Howard, J. Appl. Phys. **76**, 1633 (1994).

[2] M. V. Ramana Murty *et al.*, Phys. Rev. Lett. **80**, 4713 (1998).

[3] G. W. Lewis *et al.*, Nucl. Instrum. Methods **170**, 363 (1980).

[4] S. Rusponi, C. Baragno, and U. Valbusa, Phys. Rev. Lett. **78**, 2795 (1997).

[5] E. Chason *et al.*, Phys. Rev. Lett. **72**, 3040 (1994).

[6] G. Carter and V. Vishnyakov, Phys. Rev. B **54**, 17 647 (1996); J. Erlebacher and M. J. Aziz, Mater. Res. Soc. Symp. Proc. **440**, 461 (1997); Z. X. Jiang and P. F. A. Alkemade, Appl. Phys. Lett. **73**, 315 (1998).

[7] E. Chason, M. B. Sinclair, J. A. Floro, J. A. Hunter, and R. Q. Hwang, Appl. Phys. Lett. **72**, 3276 (1998).

[8] R. M. Bradley and J. M. E. Harper, J. Vac. Sci. Technol. A **6**, 2390 (1988); R. Cuerno and A.-L. Barabasi, Phys. Rev. Lett. **74**, 4746 (1995); M. A. Makeev and A.-L. Barabasi, Appl. Phys. Lett. **71**, 2800 (1997).

[9] The ion beam operated at 1.9×10^{-5} Torr. Incident ion fluxes of non-neutrals ranged from 0.2 to 0.7 $\mathrm{mA/cm^2}$. Temperature was maintained by a combination of backside and resistive heating. In order to eliminate contamination over the long run times from nonsample sources, samples were apertured using silicon wafers. The effect of the sputtering in this geometry was cut a wide, deep groove in the sample of the order of 1 cm wide and 10–100 μm deep. Ripples developed in this groove and could be seen by the naked eye as a diffraction grating.

[10] The peak of the blackbody spectrum was calibrated against an optical pyrometer and thermocouples.

[11] J. M. Elson, Phys. Rev. B **30**, 5460 (1984).

[12] We found no significant change in the light scattering spectra upon quenching the sample from the experimental temperature to room temperature and upon subsequent exposure to atmosphere.

[13] The temperatures at which these experiments were performed are high enough that amorphization does not occur.

[14] P. Sigmund, J. Mater. Sci. **8**, 1545 (1973).

[15] W. W. Mullins, J. Appl. Phys. **30**, 1 (1959); C. Herring, in *The Physics of Powder Metallurgy*, edited by W. E. Kingston (McGraw-Hill, New York, 1951), Chap. 8.

[16] Values for all other parameters are $n = 0.05$ atoms/Å^3, $a = 29$ Å, $Y_0(\theta = 67.5°) = 0.92$ atoms/ion, $\Gamma_2(\theta = 67.5°) = -0.0634$, and $\gamma = 1.23$ J/m^2.

[17] M. E. Keeffe, C. C. Umbach, and J. M. Blakely, J. Phys. Chem. Solids **55**, 965 (1994).

[18] M. Krueger, B. Borovsky, and E. Ganz, Surf. Sci. **385**, 146 (1997); B. S. Swartzentruber, Phys. Rev. Lett. **76**, 459 (1996); B. S. Swartzentruber, A. P. Smith, and H. Johnson, Phys. Rev. Lett. **77**, 2518 (1996).

[19] R. M. Tromp and M. Mankos, Phys. Rev. Lett. **81**, 1050 (1998).

[20] J. Y. Cavaille and M. Dreschler, Surf. Sci. **75**, 342 (1978).

[21] D. E. Jesson, K. M. Chen, S. J. Pennycook, T. Thundat, and R. J. Warmack, J. Electron. Mater. **26**, 1039 (1997).

[22] P. Nozieres and F. Gallet, J. Phys. (Paris) **48**, 353 (1987).